PAPER

www.rsc.org/loc

Efficient electrospray ionization from polymer microchannels using integrated hydrophobic membranes

Ying-Xin Wang,[a] Jon W. Cooper,[b] Cheng S. Lee[c] and Don L. DeVoe*[a]

[a] *Department of Mechanical Engineering, and Bioengineering Program, University of Maryland, College Park, USA*

[b] *Calibrant Biosystems, Rockville, MD, USA*

[c] *Department of Chemistry and Biochemistry, University of Maryland, College Park, USA*

Received 24th February 2004, Accepted 31st March 2004
First published as an Advance Article on the web 28th April 2004

A simple process for realizing stable and reliable electrospray ionization (ESI) tips in polymer microfluidic systems is described. The process is based on the addition of a thin hydrophobic membrane at the microchannel exit to constrain lateral dispersion of the Taylor cone formed during ESI. Using this approach, ESI chips are shown to exhibit well-defined Taylor cones at flow rates as low as 80 nL min^{-1} through optical imaging. Furthermore, stable electrospray current has been measured for flow rates as low as 10 nL min^{-1} over several hours of continuous operation. Characterization of the electrospray process by optical and electrical monitoring of fabricated ESI chips is reported, together with mass spectrometry validation using myoglobin as a model protein. The novel process offers the potential for low-cost, direct interfacing of disposable polymer microfluidic separation platforms to mass spectrometry.

Introduction

Microfluidic systems offer the potential for performing liquid-phase biomolecular separations with increased throughput and sensitivity while significantly reducing cost. For example, microchip separation devices which employ capillary electrophoretic and chromatographic techniques for bioseparations have been investigated extensively.[1–8] Ultimately, high resolution molecular analysis requires the coupling of these microchannel separations with mass spectrometry (MS) for accurate mass identification. Electrospray ionization (ESI), which utilizes a strong local electric field to transfer ions from solution to the gas phase in a fine spray at atmospheric pressure, is a promising approach for interfacing microfluidics to mass spectroscopy, either by direct ESI-MS interfacing, or by ESI deposition of analytes onto a matrix-assisted laser desorption ionization (MALDI) target for further MALDI-MS analysis.

Various approaches to fabricating ESI interfaces into microfluidic systems have been reported by a number of groups. External interfaces have been demonstrated by inserting capillary spray tips into microchannel exits,[9–17] or by using a liquid junction to couple the microfluidic devices to capillary-based separation systems followed by capillary ESI-MS.[18] Although these techniques have shown excellent electrospray performance, they are not fully integrated with the microfluidic channels and thus suffer from large dead volumes which can lead to broadening of separation bands, and difficulty with fabricating high density electrospray tip arrays.

Another method explored by several groups uses the flat surface at the microchannel exit, defined by cutting the substrate to expose the channel opening, to create the electrospray emitter. While straightforward, this approach leads to difficulty in consistently establishing well defined, stable Taylor cones at the microchannel exit due to liquid spreading, even for hydrophobic surfaces such as glass.[19–21] In addition to increasing Taylor cone volume, liquid spreading at the exit also limits the ability to realize tightly spaced arrays of multiple ESI tips, since crosstalk between adjacent channels poses a significant problem.

Several approaches have been explored to improve the stability of the electrospray process while also reducing exit spreading for integrated microchip ESI devices. For example, shaped spray tips have been fabricated from the bulk substrate material at the channel exit, using silicon[22] and various polymers.[23–28] Similarly, the addition of thin parylene tips bonded at the channel exit to form a wicking structure has also been demonstrated with excellent results.[29] In general, shaped tips have been shown to significantly reduce or eliminate liquid spreading and provide very good spray stability, but are relatively difficult to fabricate, requiring additional fabrication steps including mechanical machining of the substrate or the use of additional lithographically-patterned material layers in the microfluidic system.

A simpler method for improving the performance of integrated ESI tips involves increasing the hydrophobicity of the channel exit, either by application of a surface coating, or by using polymer substrates with high native hydrophobicity. The latter approach has been shown to limit liquid spreading and assist in maintaining relatively small Taylor cone volumes, but does not prevent drift in the position of the Taylor cone away from the channel exit.[21] In addition, for the case of thin film hydrophobic coatings, damage to the coating during the electrospray process can occur. For example, using a monolayer of (n-octyl) covalently-attached to the exit surface of a glass microchip, stable electrospray was limited to under 5 min at a flow rate between 100–200 nL min^{-1} before the coating was damaged.[19] Similarly, CF_4 exposure in an rf plasma system has been shown to increase the hydrophobicity of laser-shaped polycarbonate (PC) ESI tips[24] for reduced liquid spreading and improved ESI stability. However, the longevity of CF_4 plasma surface modifications is usually quite limited, typically less than 20 min based on our experience with treated PC substrates. An alternate method for forming a strongly hydrophobic coating with improved longevity has been demonstrated using a thick coating of silicon grease on the exit surface,[19] but reproducibility issues may ultimately limit the suitability of this method for broader use.

A new technique is reported here to achieve highly stable electrospray from the flat edge of a polymer microfluidic chip through the relatively simple addition of a porous hydrophobic membrane to the channel exit surface. The porous membrane provides a highly controllable and repeatable hydrophobic surface to constrain lateral dispersion of liquid from the tip exit. In addition, the resulting porous structure has the potential to act as a dense array of nanoscale ESI tips, enabling the generation of stable electrospray at exceptionally low flow rates. This concept has been demonstrated using PC microfluidic chips with poly-tetrafluoroethylene (PTFE) membranes secured to the exit surface through thermal bonding. Using this process, well-defined Taylor cones have been observed at flow rates as low as 80 nL min^{-1}, while

DOI: 10.1039/b402825b

stable electrospray current has been measured for flow rates as low as 10 nL min^{-1}.

Experimental section

Materials and reagents. Acetic acid and methanol were obtained from Fisher Scientific (Fair Lawn, NJ). Distilled water was deionized to between 16–18 MΩ cm using a Milli-Q system from Millipore (Bedford, MA). Myoglobin for ESI-MS testing was purchased from Sigma (St. Louis, MO). PTFE membrane was acquired from GE Osmonics labstore (Minnetonka, MN). Polycarbonate sheets were obtained from Sheffield Plastics (Pittsburgh, PA).

Electrospray tip preparation. Planar microfluidic electrospray tips were fabricated using polymer hot embossing with a silicon template patterned by bulk Si micromachining. The channel patterns were defined in a photoresist layer spun on a 2.4 μm thick silicon dioxide surface of a 10 cm diameter < 100 > oriented p-type silicon wafer (Silicon Quest International, Reno, NV). The patterned wafer was then etched with buffered hydrofluoric acid solution to define openings to the bulk Si surface. The Si was then etched to a depth of 30 μm in a potassium hydroxide solution to form the embossing mold. The resulting template was used to imprint PC substrates in a customized hot press (AutoFour/15-P hydraulic press, Carver, Wabash, IN) to form microfluidic channels with trapezoidal cross section (120 μm wide at the top, 80 μm wide at the bottom, 30 μm deep, 4.5 cm long). The imprinted substrate was then thermally bonded with a blank PC substrate in which a reservoir hole was drilled for electrical and fluidic access to the channel.

Once the channel is sealed, the resulting chip is cut to define the emitter tip using a tabletop bandsaw (MicroLux, Micro-Mark, Berkeley Heights, NJ) and a CNC machining system (MicroMill 2000 HD/LE, MicroProto Systems, Chandler, AZ). Mechanical cutting was found to produce an exit surface with average roughness of 12 μm as measured with a stylus profilometer (XP2, Ambios Technology, Santa Cruz, CA). However, this high roughness was not found to affect the final spray tip performance. After checking that the machined microchannel exit is not clogged or deformed during machining, a 50 μm thick PTFE membrane with porosity of 70% and average pore size of 0.22 μm is placed over the channel exit and secured in place by fixing a glass cover slide to the exposed side of the membrane. The glass/membrane/chip assembly is then placed on a digital hotplate (Dataplate PMC 730, Barnstead International, Dubuque, IA) set just above the glass transition temperature of the PC chip (~150 °C) while manually applying a low force of approximately 40 N for 10 s, allowing the PC substrate to permanently bond to the adjacent membrane surface without substantially deforming the channel exit. Capillary connections (nanoport, Upchurch Scientific, Oak Harbor, WA) were bonded with epoxy on top of the reservoir to provide liquid supply from the syringe pump. A platinum electrode contacting the liquid through a capillary T-junction (Upchurch Scientific) provides the required electrical contact for ESI.

Optical observations of the electrospray ionization process were performed using an experimental setup assembled on a probe station (Cascade REL-4800, Cascade Microtech, Beaverton, OR). The electrospray voltage was delivered to the platinum electrode using a high voltage power supply (CZE 1000R, Spellman High Voltage Electronics, Plainview, NY). Total ion current generated from the spray between the tip and a polished aluminium plate held at a fixed distance from the tip was obtained from a multimeter (34401A, Agilent, Palo Alto, CA) by measuring the voltage across a 100 kΩ resistor. A 500 μL gastight syringe driven by a syringe pump (PHD2000, Harvard Apparatus, Holliston, MA) delivered buffer solution of 50% water, 49% methanol, and 1% acetic acid (pH ~ 3.6) to the emitter. The electrospray ionization process was observed through a microscope (FS-70, Mitutoyo, Japan) with objectives ranging from 2–100× and captured using a CCD video camera. The precise 3-D positioning between the polished aluminium ground plate and the emitter was realized using a probe station micropositioner, and the emitter-to-counterelectrode distance was determined through a reticle in the microscope eyepiece calibrated by a stage micrometer.

Results and discussions

Device fabrication. Fig. 1(a) shows a typical PC electrospray chip fabricated by hot embossing from a silicon master. The chip contains a single microchannel with an average width of 100 μm and depth of 30 μm, running lengthwise from the input reservoir to the leftmost edge as shown in this figure (a length of 4.5 cm). Fig. 1(b) is a photomicrograph of the electrospray exit surface with an approximately rectangular (2.5 × 1.5 mm) section of 50 μm thick PTFE membrane bonded to the exit. The dark regions of the membrane correspond to areas where excessive force during bonding produced optically transparent patches due to collapse of the membrane pores, while the light region reflects successful bonding without pore collapse. The higher forces in the collapsed regions are believed to result from ridges in the PC substrate formed by the end milling process used to create the exit surface, which tend to compress the membrane along the protruding edges.

Fig. 2 shows scanning electron micrographs of the membrane (a) prior to bonding, and (b) after thermal bonding to the microchannel exit. The original membrane has a tortuous structure with an average pore size of 0.22 μm as reported by the manufacturer. The average pore size and surface pore distribution were found to be modified during thermal bonding due to the bonding force and high temperature, with moderate reduction in porosity observed. No significant change to the membrane surface was observed following continuous testing for up to 4 h. After 4 h, however, some

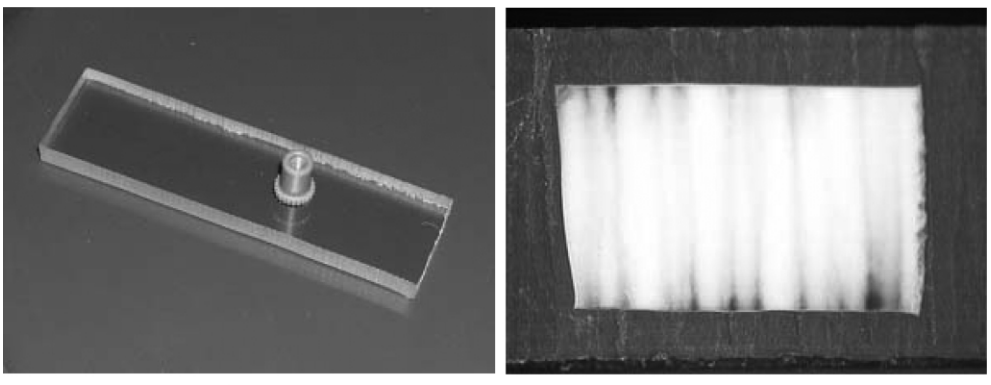

(a) (b)

Fig. 1 (a) Typical PC/PTFE electrospray chip used for characterization, and (b) photomicrograph of PTFE patch bonded to exit surface of electrospray chip.

damage to the external surface of the membrane often occurred. Following 6 h of continuous operation, many of the smaller pores on the PTFE surface can become sealed. Despite the damage to the membrane surface, the nanoscale pores within the interior of the membrane generally exhibit little or no damage.

Optical ESI characterization. Electrospray behavior and Taylor cone geometry was observed under the microscope, with the corresponding total ion current from the emitter exit simultaneously measured. The analyte (myoglobin, 1 mg mL^{-1}) in a buffer solution of 50% water, 49% methanol, and 1% acetic acid was filled into the microchannel and sprayed directly from the channel exit through the bonded PTFE membrane towards the ground plate. The electrospray voltage was applied through a platinum electrode interfaced *via* a T-junction located at the input reservoir 45 mm from the microchannel exit.

For plain PC microchannel exits without a bonded membrane, liquid exiting the channel was observed to rapidly wet a large area of the flat edge surface, thereby preventing generation of stable electrospray. In contrast, for chips with PTFE membranes bonded at the channel exits, liquid exiting the chips consistently formed small rounded droplets aligned to the channels, without no liquid expansion observed. When the ESI voltage was applied and slowly increased, the droplet elongated and formed into an elliptically-shaped cone. As the voltage was further increased to a threshold voltage, the ellipsoid spontaneously changed to a pointed cone and the electrospray started, as evidenced by the measurement of a jump in ion current between the ESI chip and polished ground plate. Threshold voltages of 3200 and 3520 V were measured for 1.5 and 2 mm microchip-to-counterelectrode spacings, respectively. As the counterelectrode spacing increased, the threshold voltage increased since the electrical field exhibits a logarithmic dependence on the separation distance for small gaps. As expected, the threshold voltage increases with higher gaps. Typically, electrospray was found to be stable for between 4–6 h, as evidenced by stable ion current measurements during this time period.

Fig. 3 shows optical images of stable Taylor cone-jets established at a microchannel exit with different applied voltages at a flow rate of 120 nL min^{-1} and counter electrode spacing of 2 mm. As the applied voltage increased, the Taylor cone size decreased, with an associated decrease in jet diameter and jet breakup length. As expected, we also observed that as the flow rate decreased, the Taylor cone size also decreased. As can be seen in this figure, the cones are well defined with virtually no lateral dispersion from the microchannel exit.

Electrical ESI characterization. Current/voltage (*I*/*V*) characteristics were measured for fabricated ESI chips as a function of applied flow rate and chip-to-counterelectrode spacing. Fig. 4 shows the effect of flow rate on the *I*/*V* curve. For a set flow rate, the current increases with increasing applied voltage. At a constant applied voltage, the current increases as the flow rate increases. The current can be predicted by approximate equations derived from theoretical and semi-empirical models, *e.g.*, refs. 30–33. In particular, the current increases exponentially with the volume flow rate (V_f) of the solution, $I \propto (V_f)^n$. In our experiments, the value of n was found to be approximately 0.55 to give a fair correspondence of currents at different flow rates. Note that at flow rates lower than 80 nL min^{-1}, the Taylor cone was not visible under the microscope.

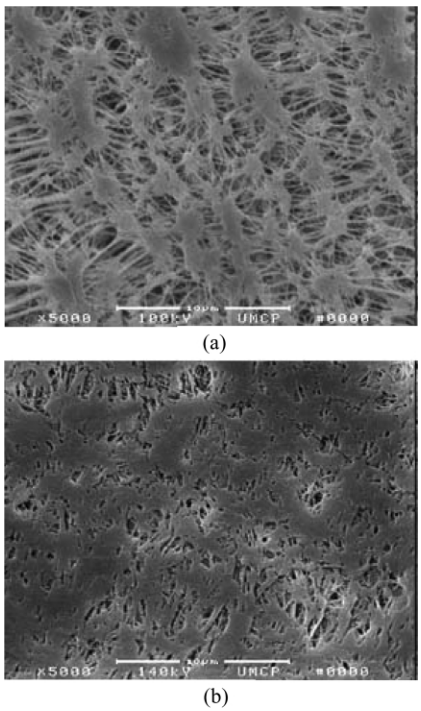

Fig. 2 SEM images of PTFE surface (a) before bonding, (b) after bonding.

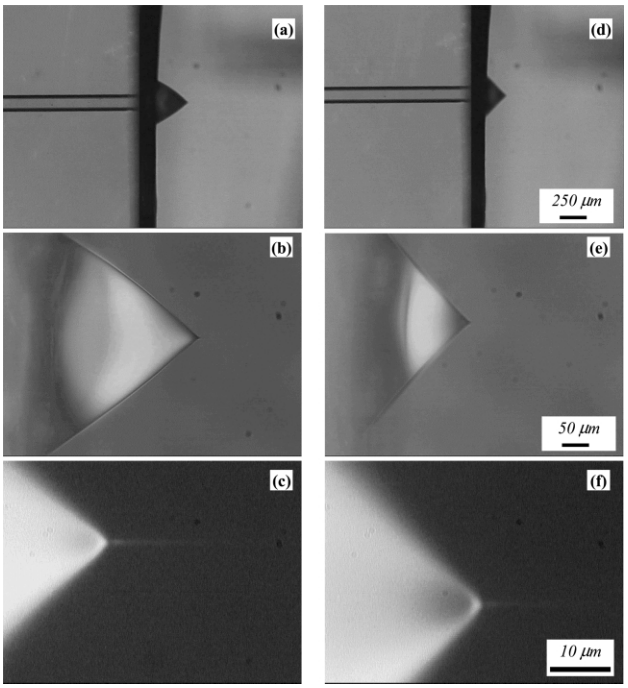

Fig. 3 Photomicrographs of stable Taylor cones established at microchannel exit for a flow rate of 120 nL min^{-1} and chip-to-counterelectrode spacing of 2 mm. The applied voltage for images (a)–(c) is 3800 V, and for images (d)–(f) is 4000 V.

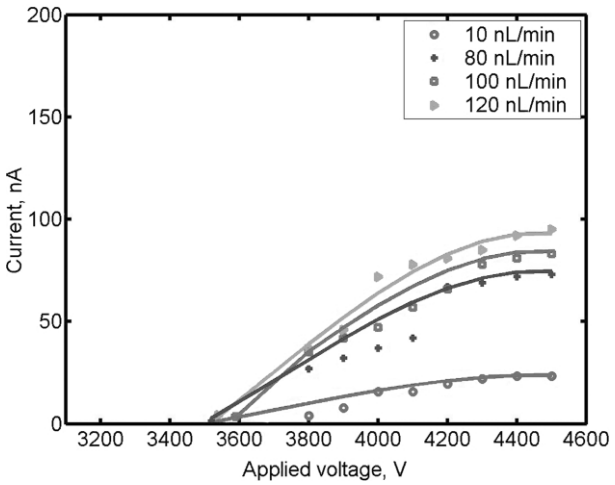

Fig. 4 Measured electrospray current as a function of applied voltage at different flow rates (2 mm chip-to-counterelectrode spacing).

However, stable electrospray current was obtained for flow rates as low as 10 nL min^{-1}, as shown in Fig. 4. Fig. 5 shows the effect of channel exit-to-counter electrode spacing on current-voltage relation. At the same flow rate, the current is higher for the smaller chip-to-counterelectrode spacing. As can be seen, the threshold voltage at 1.5 mm is smaller than that at 2 mm due to the stronger electric field. Note that fabricated chips have shown good repeatability in electrospray behavior. More than 20 chips have been fabricated and tested, with no significant differences in electrospray performance between different chips operated continuously for 6 h.

ESI-MS validation. To evaluate the utility of the PC/PTFE electrospray method, a test chip was fixed onto a micromanipulator and positioned such that the outlet end of the electrospray channel was approximately 3 mm in front of, and 3 mm away from, the orifice of a mass spectrometer (Qtof Micro, Micromass). Using a syringe pump, Myoglobin (16.9 kDa) at a concentration of 0.5 mg mL^{-1} was infused through the electrospray chip at a constant flow rate of 100 nL min^{-1}, until forming a droplet on the exterior surface of the PTFE membrane. Electrospray was performed with application of 3.7 kV at the T-junction. Spectra were collected with a scan range of 700–1200 Da, and a scan time of 0.9 s (1 scan). The amount of analyte consumed during this test was approximately 60 fmol. The resulting spectrum exhibits the expected protein charge envelope characteristic of myoglobin, as shown in Fig. 6.

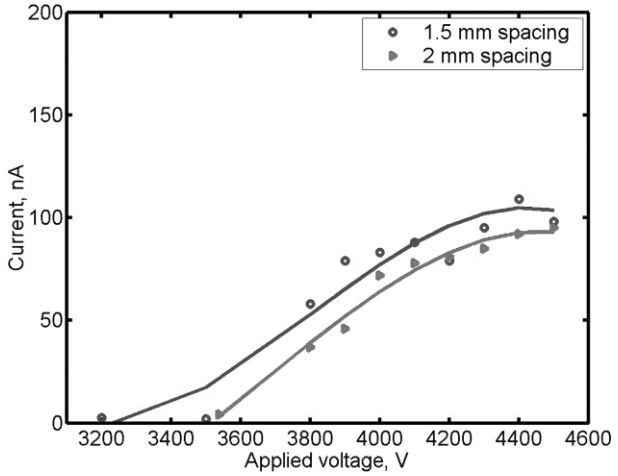

Fig. 5 Measured electrospray current as a function of applied voltage for different chip-to-counterelectrode spacings (120 nL min^{-1} flow rate).

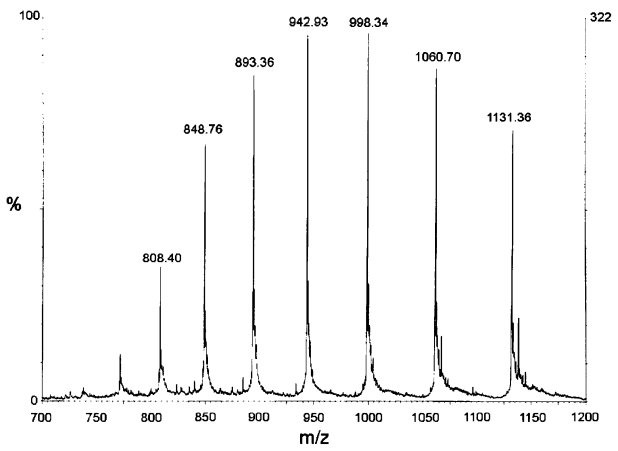

Fig. 6 Protein charge envelope for myoglobin (0.5 mg mL^{-1}) measured by ESI-MS from the electrospray chip at a flow rate of 100 nL min^{-1}.

Conclusions

Confined electrospray from the flat edges of planar microfluidic chips has been demonstrated through the addition of hydrophobic PTFE membranes bonded to the exit surfaces. The effects of applied potential, flow rate, and chip-to-counterelectrode spacing on ESI performance follow expected theoretical trends. The technique offers the potential for direct, stable, and repeatable interfacing between polymer microfluidic systems and mass spectrometry, without requiring significant additional fabrication effort. While a 50 μm thick PTFE membrane with 0.22 μm average pore size was used in this work to consistently achieve well-defined and stable Taylor cones with no lateral spreading on PC substrates, the concept is portable to microfluidic systems based on other rigid polymers with glass transition temperatures below that of the PTFE membrane.

Acknowledgements

The authors gratefully acknowledge support for this research from the National Institutes of Health through NCI grant CA092819, and from the Defense Advanced Research Projects Agency (DARPA) through contract DAAH01-03-C-R182.

References

1 D. J. Harrison, A. Manz, Z. Fan, H. Ludi and H. M. Widmer, *Anal. Chem.*, 1992, **64**, 1908–1919.
2 D. J. Harrison, K. Fluri, K. Seiler, Z. Fan, C. S. Effenhauser and A. Manz, *Science*, 1993, **261**, 895–897.
3 C. S. Effenhauser, A. Manz and H. M. Widmer, *Anal. Chem.*, 1993, **65**, 2637–2642.
4 S. C. Jacobson, R. Hergenroder, L. B. Koutny and J. M. Ramsey, *Anal. Chem.*, 1994, **66**, 2369–2373.
5 H. Becker, K. Lowack and A. Manz, *J. Micromech. Microeng.*, 1998, **8**, 24–28.
6 J. Han and H. G. Craighead, *Science*, 2000, **288**, 1026–1029.
7 R. D. Rocklin, R. S. Ramsey and J. M. Ramsey, *Anal. Chem.*, 2000, **72**, 5244–5249.
8 N. Gottschlich, S. C. Jacobson, C. T. Culbertson and J. M. Ramsey, *Anal. Chem.*, 2001, **73**, 2669–2674.
9 N. H. Bings, C. Wang, C. D. Skinner, C. L. Colyer, P. Thibault and D. J. Harrison, *Anal. Chem.*, 1999, **71**, 3292–3296.
10 I. M. Lazar, R. S. Ramsey, S. Sundberg and J. M. Ramsey, *Anal. Chem.*, 1999, **71**, 3627–3631.
11 L. Licklider, X. Wang, A. Desai, Y. Tai and T. D. Lee, *Anal. Chem.*, 2000, **72**, 3627–3631.
12 J. H. Chan, A. T. Timperman and R. Aebersold, *Anal. Chem.*, 1999, **71**, 4437–4444.
13 J. Li, J. F. Kelly, I. Chernushevich, D. J. Harrison and P. Thibault, *Anal. Chem.*, 2000, **72**, 599–609.
14 Y. Jiang, P. Wang, L. E. Locascio and C. S. Lee, *Anal. Chem.*, 2001, **73**, 2048–2053.
15 D. Figeys and R. Aebersold, *Anal. Chem.*, 1998, **70**, 3721–3727.
16 N. Xu, Y. H. Lin, S. A. Hofstadler, D. Matson, C. J. Call and R. D. Smith, *Anal. Chem.*, 1998, **70**, 3553–3556.
17 Z. Meng, S. Qi, S. A. Soper and P. A. Limbach, *Anal. Chem.*, 2001, **73**, 1286–1291.
18 J. Kameoka, H. G. Craighead, H. Zhang and J. Henion, *Anal. Chem.*, 2001, **73**, 1935–1941.
19 Q. Xue, F. Foret, Y. M. Dunayevskiy, P. M. Zavracky, N. E. McGruer and B. L. Karger, *Anal. Chem.*, 1997, **69**, 426–430.
20 R. S. Ramsey and J. M. Ramsey, *Anal. Chem.*, 1997, **69**, 1174–1178.
21 T. C. Rohner, J. S. Rossier and H. H. Girault, *Anal. Chem.*, 2001, **73**, 5353–5357.
22 G. A. Shultz, T. N. Corso, S. J. Prosser and S. Zhang, *Anal. Chem.*, 2000, **72**, 4058–4063.
23 C. Yuan and J. Shiea, *Anal. Chem.*, 2001, **73**, 1080–1083.
24 K. Tang, Y. Lin, D. W. Matson, T. Kim and R. D. Smith, *Anal. Chem.*, 2001, **73**, 1658–1663.
25 J. Wen, Y. Lin, F. Xiang, D. W. Matson, H. R. Udseth and R. D. Smith, *Electrophoresis*, 2000, **21**, 191–197.
26 J. Kim and D. R. Knapp, *J. Am. Soc. Mass Spectrom.*, 2001, **12**, 463–469.

27 J. Kim and D. R. Knapp, *Electrophoresis*, 2001, **22**, 3993–3999.
28 V. Gobry, J. Van Oostrum, M. Martinelli, T. C. Rohner, F. Reymond, J. S. Rossier and H. H. Girault, *Proteomics*, 2002, **2**, 405–412.
29 J. Kameoka, R. Orth, B. Ilic, D. Czaplewski, T. Wachs and H. G. Craighead, *Anal. Chem.*, 2002, **74**, 5897–5901.
30 D. P. H. Smith, *IEEE Trans. Ind. Appl.*, 1986, **IA-22**, 527–535.
31 I. Hayati, A. I. Bailey and T. F. Tadros, *J. Colloid Interface Sci.*, 1987, **117**, 205.
32 J. Fernandez de la Mora and I. G. Locertales, *J. Fluid Mech.*, 1994, **243**, 561.
33 M. S. Wilm and M. Mann, *Int. J. Mass Spectrom. Ion Processes*, 1994, **136**, 167–180.